Available online at www.sciencedirect.com

SciVerse ScienceDirect

journal homepage: www.elsevier.com/locate/he

Controllable proton and CO_2 photoreduction over Cu_2O with various morphologies

*Albertus D. Handoko, Junwang Tang**

Department of Chemical Engineering, University College London, Torrington Place, London WC1E 7JE, United Kingdom

ARTICLE INFO

Article history:
Received 5 January 2013
Received in revised form
22 March 2013
Accepted 26 March 2013
Available online 25 April 2013

Keywords:
Solar energy
CO_2 reduction
Cu_2O photocatalyst
Heterojunction

ABSTRACT

Simultaneous photocatalytic reduction of water to H_2 and CO_2 to CO was observed over Cu_2O photocatalyst under both full arc and visible light irradiation (>420 nm). It was found that the photocatalytic reduction preference shifts from H_2 (water splitting) to CO (CO_2 reduction) by controlling the exposed facets of Cu_2O. More interestingly, the low index facets of Cu_2O exhibit higher activity for CO_2 photoreduction than high index facets, which is different from the widely-reported in which the facets with high Miller indices would show higher photoactivity. Improved CO conversion yield could be further achieved by coupling the Cu_2O with RuO_x to form a heterojunction which slows down fast charge recombination and relatively stabilises the Cu_2O photocatalyst. The RuO_x amount was also optimised to maximise the junction's photoactivity.

1. Introduction

Our world is facing complex and intertwined issues on pollution and energy. Rapid economic growth promotes insatiable demand for energy, causing spikes in energy prices coupled with depleting natural resources. At the same time, consumption of energy, fossil fuels in particular, contributes significantly to the increase of greenhouse gases such as CO_2. Many strategies were proposed, but a viable solution requires the utilisation of a renewable energy source and low (initial and running) costs. Photochemical reduction of CO_2 to fuels or value-added chemicals using inorganic semiconductor is an attractive solution for both rising demand for clean energy and the need for greenhouse gas reduction.

Cu_2O is a cheap, relatively abundant and intrinsically *p*-type semiconductor with a low bandgap of about 2–2.2 eV [12,13]. In theory, the narrow bandgap and appropriate positioning of the conduction and valence bands make Cu_2O an ideal photocatalyst for water splitting and CO_2 reduction. It is acknowledged that Cu_2O has photo-stability issue that remains a challenge [11,16]. Several correlation studies between photocatalytic reduction activity (of water to H_2) on various Cu_2O exposed facets have been reported previously [22,23], indicating that unconventional Cu_2O shapes consisting mostly of high-index facets display significantly higher activities than conventional ones (cubes, etc.) with mainly low-index facets. We very recently found that Cu_2O is an appropriate candidate photocatalyst for CO_2 photoreduction driven by visible light [4]. It is very interesting to observe the influence of Cu_2O facets on CO_2 photoreduction and the correlation between different Cu_2O shapes and product selectivity between water and CO_2 photoreduction. In this paper, the morphology/exposed Cu_2O facets were tuned and the photocatalytic reactions were investigated in an aqueous suspensions system. Tuneable product selectivity was observed and discussed. Finally, heterojunction of RuO_x/Cu_2O was optimised to improve Cu_2O photoactivity.

* *Corresponding author*. Fax: +44 020 7383 2348.
E-mail address: junwang.tang@ucl.ac.uk (J. Tang).

0360-3199/$ – see front matter
http://dx.doi.org/10.1016/j.ijhydene.2013.03.128

2. Experimental

Two types of Cu_2O powders used in this study, cuboid and octahedral-shaped, were prepared using solvothermal method. Typical synthesis of cuboid-shaped Cu_2O involves the dissolution of $Cu(NO_3)_2 \cdot 2.5H_2O$ in a PTFE lined hydrothermal reactors containing ethanol-water mixture (64:36 volume ratio), and formic acid (1.3 M). Octahedral-shaped Cu_2O was synthesised by adding 0.65 M of NH_4OH. Deep red/purple precipitates obtained after 2 h reaction at 145 °C were washed repeatedly (5–6 times) with copious amount of water (50 ml) and dried in an convection oven (70 °C) overnight. Different Cu_2O-RuO_x junctions were prepared by impregnation method using appropriate $RuCl_3 \cdot xH_2O$ concentration in water followed by heat treatment then washed for a final time and let to dry at 70 °C before finally heated at 200 °C for 3 h.

Powder XRD was performed using Panalytical X'Pert powder diffraction system fitted with X'cellerator scanning linear detector in 0.0167° steps, at 10 s acquisition time per step. The incident X-ray is nickel filtered Cu radiation ($CuK_{\alpha 1}$: 1.540596 Å, $CuK_{\alpha 2}$: 1.544493 Å, $CuK_{\alpha 1}/CuK_{\alpha 2}$ ratio *ca.* 65/35). Particle morphology was observed using JEOL-7400 high resolution field emission electron microscope operated at 3 kV accelerating voltage and 10 mA current 0° stage tilt on gold coated powders. TEM measurements were conducted using JEOL-2000-EX-MKII transmission electron microscope (200 kV). Ten points adsorption-desorption tests on the powder samples were performed on Micromeritics® TriStar 3000 with N_2 carrier gas to get an estimate of their surface area using BET calculation method.

CO_2 reduction reaction was carried out in photocatalyst suspension system using septa-sealed glass chambers fit with flat borosilicate top window (>90% transmittance for $\lambda \geq 350$ nm). Prior to measurements, Cu_2O powders and glass chamber were treated at 200 °C for 3 h in a convection oven and under 300 W Xe lamp light source for *ca.* 1 h to remove traces of organic contaminants. A typical photocatalytic experiment is conducted using 0.5 g of photocatalyst in 3 ml of CO_2 saturated deionised H_2O (Elga Centra). Excess (0.7 M) sodium sulphite was added in each run as hole scavenger while deionised H_2O was being purged with CO_2, to achieve close to neutral condition (pH ≈ 7.6) before introducing the Cu_2O photocatalyst. 150 W Xe lamp (Newport) was used as a light source. Various long pass filters (Comar Instruments) were applied to evaluate the visible light activity. The reaction products were monitored by periodical sampling of the gas phase from the glass chambers using a gas tight syringe to a gas chromatograph (Varian GC-450) fit with thermal conductivity detector (TCD) connected to molecular sieve column to detect H_2, CO_2, O_2 and N_2 and flame ionization detector (FID) connected to CP-SIL 5CB (Varian) capillary column to detect hydrocarbons. Argon was used as the GC carrier gas. A methaniser was installed to enable the FID to detect CO and CO_2 with 1000× higher sensitivity.

3. Results and discussions

Representative XRD data of both Cu_2O powders morphologies are shown in Fig. 1. While all peaks can be matched with the standard Cu_2O reference [7], octahedral-Cu_2O (Fig. 1a) displayed much sharper and more intense peaks compared to the cuboid-Cu_2O (Fig. 1b), suggesting much larger crystallite size. It was also noticed that the intensity ratio between the (111) and (002) reflexions for octahedral-Cu_2O was much higher at 3.3 vs. 2.9 for cuboid-Cu_2O. This indicates a pronounced {111} preferred orientation on octahedral-Cu_2O which are not seen on cuboid-Cu_2O.

Fig. 2 shows the different morphologies of as-grown Cu_2O. In line with the findings from XRD, it was observed that the octahedral-Cu_2O particles were larger than the cuboid-Cu_2O (Fig. 2a), in excess of 10 μm (Fig. 2c). Each octahedral displays eight uniform faces, which can be assigned to the Cu_2O {111} plane according to the preferred orientation found in the XRD

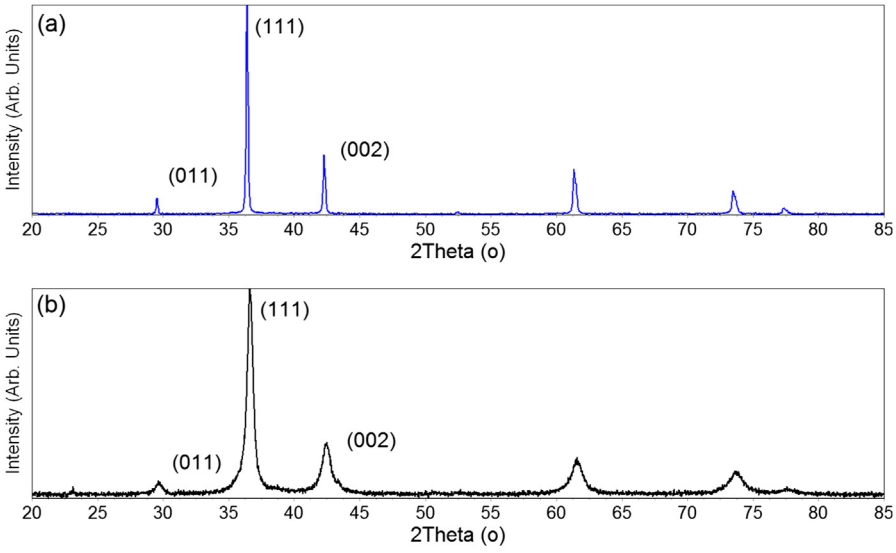

Fig. 1 – Representative XRD data of (a) octahedral-Cu_2O and (b) cuboid-Cu_2O aggregates. All peaks can be matched with standard Cu_2O reference.

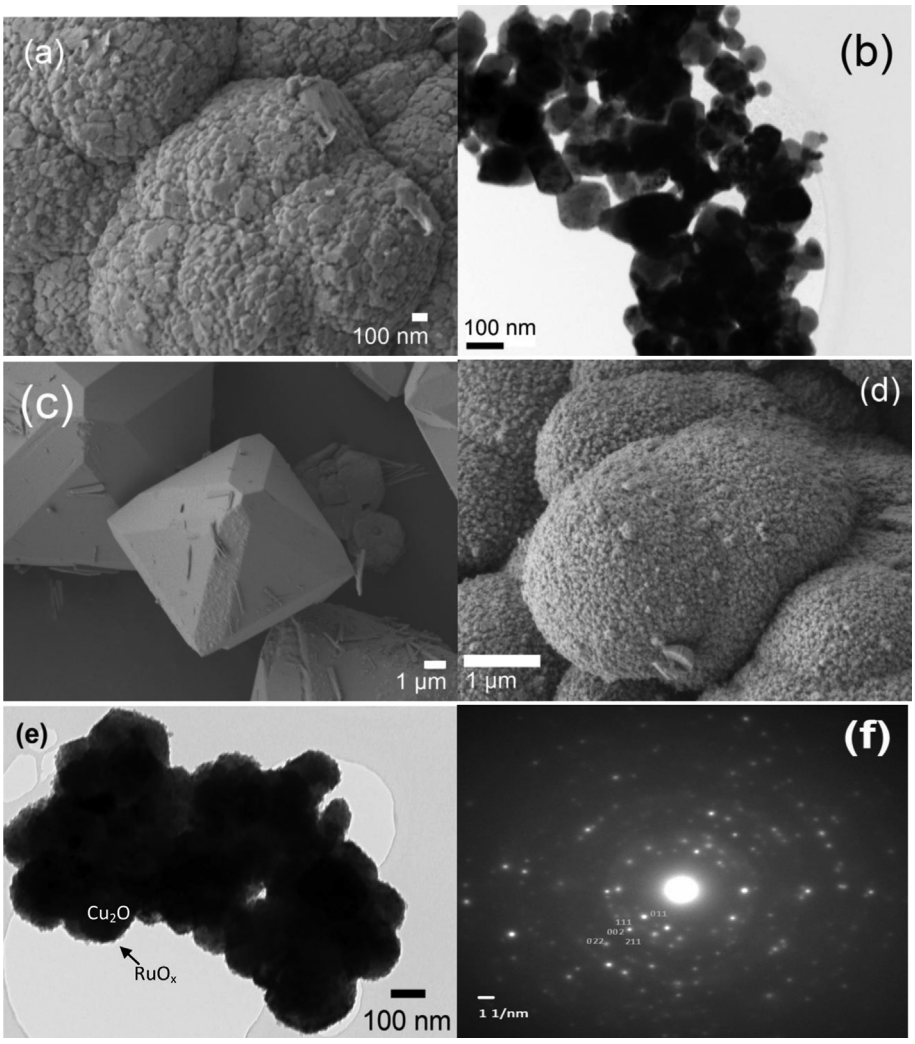

Fig. 2 – Different morphologies of as-grown Cu_2O particles or particle aggregates: (a) FESEM and (b) TEM micrographs of cuboid-Cu_2O aggregate, showing exposed {100} facets with irregular edges and corners. (c) Octahedral-shaped Cu_2O particles with exposed {111} on its eight octahedral faces. (d) FESEM and (e) TEM micrographs of RuO_x/Cu_2O heterojunction (f) Electron diffraction data of cuboid-Cu_2O TEM micrograph shown in b.

data. Cuboid-Cu_2O on the other hand, tends to form spherical aggregates of *approx.* 2 μm diameters (Fig. 2a). The BET surface area of the samples was measured, it is *ca.* 0.12 $m^2\ g^{-1}$ for octahedral Cu_2O and 0.55 $m^2\ g^{-1}$ for cuboid-Cu_2O.

It was also observed using TEM that the individual cuboid-shaped Cu_2O particles were defined as 50–100 nm particles with round edges and corners (Fig. 2b). Electron diffraction data (Fig. 2e) suggested that the six exposed faces of cuboid-Cu_2O could be assigned to the Cu_2O {002} plane, judged by the unusually bright {002} diffraction spot and much weaker {111} diffraction at the same time.

UV–Vis absorption spectra of both Cu_2O morphologies are shown in Fig. 3. While both Cu_2O morphology show similar band edge around 660 nm, although the cuboid-Cu_2O spectra were slightly blue-shifted, probably because of its smaller crystallite size. The estimated bandgaps of cuboid and octahedral-Cu_2O are *approx.* 1.87 and 1.83 eV respectively.

Despite having over four times lower surface area, octahedral-Cu_2O ({111} terminated) produces much more H_2 with

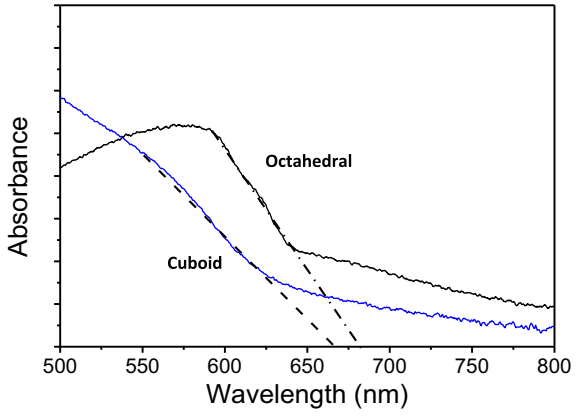

Fig. 3 – UV–Vis spectra of Cu_2O with various morphologies.

trace amounts of CO (Fig. 4a and b), indicating the surface are is not the dominating factor in the studies. Cuboid-Cu_2O aggregates ({100} terminated) on the other hand display a peculiar preference towards CO_2 reduction to CO in expense of reduced H_2 production. As the same photocatalytic reaction conditions were applied on both Cu_2O shapes, the photoreduction selectivity shift from H_2 to CO can only be attributed to the exposed Cu_2O facets taking into account the similar UV–Vis absorption of the two samples.

It has been shown previously that catalytic activity can be altered with varying catalyst shape and sizes [9]. The key argument is that the different catalyst shapes dictate the fraction of atom located on the edges, corners, or high-index facets [22]. These locations possess much greater density of unsaturated (slightly under-coordinated) steps, and imperfections like ledges, kinks compared to low indexed planes, which can serve as active sites for breaking chemical bonds [10,17,19]. In some other oxides like ZnO, higher catalytic activity could also rise from the different polarity of the exposed facets [20,21].

Reports on the use of Cu_2O for photocatalytic water splitting have always been based on tetrapod-shaped Cu_2O, which consists of mainly {111} exposed facets [5,6]. From the different photoreduction products observed in this study, it is proposed the Cu_2O {111} facets, seen on the octahedral-Cu_2O may be the dominant surface for proton reduction. The Cu_2O {100} facets and the irregular edges observed in cuboid-Cu_2O aggregates on the other hand is likely dominant for CO_2 photoreduction sites. In other words, the low index facets exhibit higher activity for CO_2 photoreduction than high index facets, which is different from the common rules mentioned in the introduction. The possible reason for this might be due to the adsorption of CO_2 on different facets of Cu_2O. More detailed studies are underway.

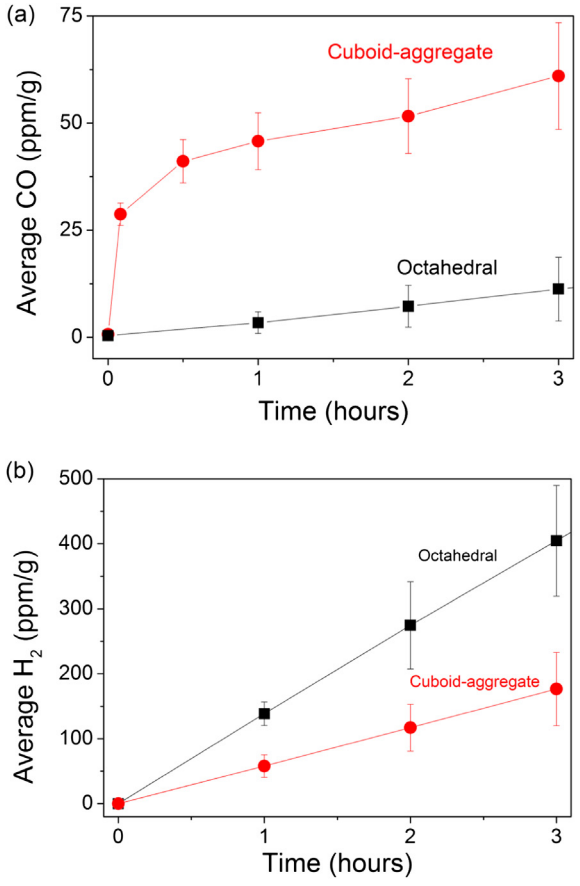

Fig. 4 – Averaged photocatalytic activity of various Cu_2O particles or aggregates (a) CO yield, (b) H_2 yield under full arc of 150 W Xe lamp. Test conditions: 0.5 g photocatalyst, 3 ml of CO_2 saturated deionised H_2O, 0.7 M Na_2SO_3 scavenger.

It was also noticed that the gas evolution rate profile of H_2 and CO were different. H_2 evolution rates for both Cu_2O morphologies are more or less linear with time (Fig. 4b), while the CO evolution rate, especially in the spherical-shaped Cu_2O, decreases after the first hour (Fig. 4a). It is possible that this is caused by differing stability of Cu_2O {111} and {100} facets in presence of aqueous sulphate as reported previously [15]. Indeed the cuboid-Cu_2O was more severely degraded after photocatalytic reactions than octahedral shaped particles (see Supporting Information Figs. S1 and S2), implying that the {111} facets seen on octahedral-shaped Cu_2O are much more stable and indeed responsible for proton reduction reactions.

Rapid charge recombination is the key issue in photocatalytic reactions over many photocatalysts [18]. It has preliminarily been observed that a solid-state heterojunction based on CuO_2 can efficiently separates holes from electrons, observed by time resolved spectroscopy [4]. Similar phenomenon was also observed on cobalt phosphate coated Fe_2O_3 photoelectrodes [1]. RuO_x is a conductive metal oxide with large work function [2,3], which has been proven effective as oxidation catalyst for many substances including water [8,14,24]. Different loading amounts of RuO_x were therefore investigated in detail herein on cuboid-shaped Cu_2O aggregates to find out the optimum RuO_x loading. The amounts of CO evolved for the first 30 min were plot in Fig. 5a. It is apparent that the photoreduction activity of the RuO_x/cuboid-Cu_2O ({100} dominated) junction generally increases with increasing RuO_x amount up to 0.25%, due to the enhanced in-situ charge separation effect. However as shown in the SEM micrograph of 0.25 wt% RuO_x/CuO_2 sample (Fig. 2d), the CuO_2 surface is nearly fully covered by RuO_x, above the amount the light screening effect by the RuO_x particulates becomes dominant. The photoactivity decreases after this point onwards until 1.5 wt% of the RuO_x loading. Furthermore, the stability of the cuboid-Cu_2O ({100} dominated) is relatively enhanced by the surface coating of RuO_x layer (see Supporting Information Figs. S1 and S3). It is also noted that the increase of CO production occurs at the expense of H_2, the H_2 production rate decreases from *ca.* 50 ppm g^{-1} h^{-1} for bare cuboid Cu_2O to around 12 ppm g^{-1} h^{-1} for 0.25% RuO_x loaded cuboid Cu_2O. This is likely because the low availability of suitable H_2 evolution sites on the cuboid Cu_2O surface is further blocked by the RuO_x loading.

Cu_2O is a narrow bandgap semiconductor. Its photoactivity was also investigated under visible light. The activities of bare and 0.25 wt% RuO_x/cuboid-Cu_2O were observed by filtering wavelengths below 420 nm using a long pass filter (Fig. 5b). The results clearly show that both bare Cu_2O and RuO_x/Cu_2O junction exhibit visible driven activity for CO_2

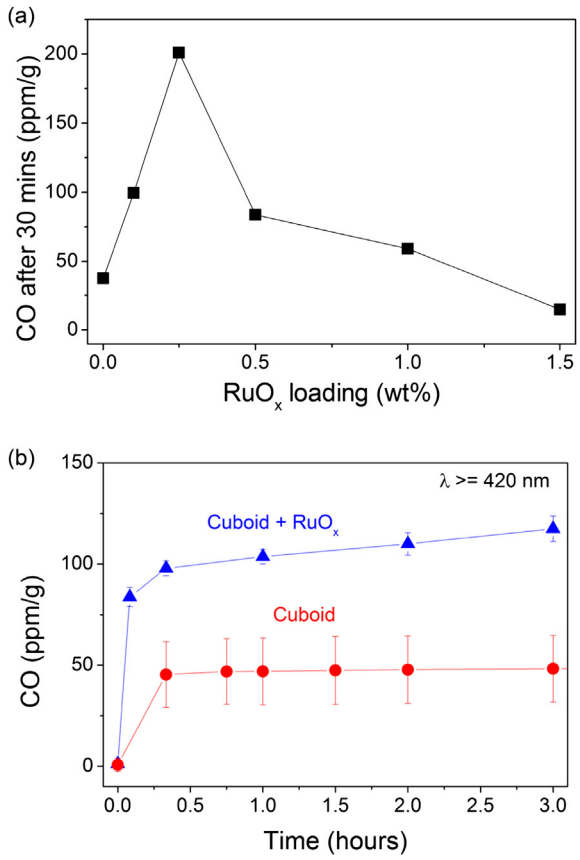

Fig. 5 – (a) The first 30 min of CO yield of cuboid-Cu_2O aggregates with different amount of RuO_x co-catalyst loading, (b) Activity of cuboid Cu_2O and the heterojunction under visible light ($\lambda \geq 420$ nm). Test conditions: 0.5 g photocatalyst, 3 ml of CO_2 saturated deionised H_2O, 0.7 M Na_2SO_3 scavenger.

photoreduction, however the RuO_x/Cu_2O is much more active than bare Cu_2O and able to sustain the CO evolution rate better after the first hour.

4. Conclusions

In summary, we highlighted that the photocatalytic reaction selectivity shifted in favour of CO_2 reduction by tuning the shape and exposed sites of Cu_2O photocatalyst. Furthermore, different from the many reports in which the facets with high Miller indices show higher photoactivity, e.g. for water splitting, low index facets of Cu_2O is beneficial for CO_2 photoreduction. It was also found that bulk Cu_2O instability is a serious issue for photocatalytic CO_2 reduction than H_2 evolution, because the {111} exposed facet that prefers H_2 evolution reaction were found to be much more stable than the {100} in aqueous solution containing sulphates. As expected RuO_x loading improves the CO evolution yield under both full arc and visible light irradiation, and the optimum loading for the cuboid-Cu_2O aggregates were found at 0.25 wt%, above which the light blocking effect from RuO_x dominates and reduce the overall photocatalytic activity.

Acknowledgements

Financial support from the EPSRC (EP/H046380/1) is gratefully acknowledged. The authors thank Dr. M. Ardakani (Imperial College London) for TEM measurements. J. Tang is also thankful for a grant from the Qatar National Research Fund under its National Priorities Research Program award number NPRP 09-328-2-122. Its contents are solely the responsibility of the authors and do not necessarily represent the official views of the Qatar National Research fund.

Appendix A. Supplementary data

Supporting information: FESEM micrograph of (S1) cuboid-Cu_2O, (S2) Octahedral-Cu_2O and (S3) heterojunction after 3 h reaction can be found online at http://dx.doi.org/10.1016/j.ijhydene.2013.03.128.

REFERENCES

[1] Barroso M, Cowan AJ, Pendlebury SR, Grätzel M, Klug DR, Durrant JR. The role of cobalt phosphate in enhancing the photocatalytic activity of α-Fe_2O_3 toward water oxidation. J Am Chem Soc 2011;133:14868–71.
[2] Chueh YL, Hsieh CH, Chang MT, Chou LJ, Lao CS, Song JH, et al. RuO_2 nanowires and RuO_2/TiO_2 core/shell nanowires: from synthesis to mechanical, optical, electrical, and photoconductive properties. Adv Mater 2007;19:143–9.
[3] de Almeida JS, Ahuja R. Electronic and optical properties of RuO_2 and IrO_2. Phys Rev B 2006;73:165102.
[4] Handoko AD, Pastor E, Reynal A, Pesci FM, Guo M, Cowan AJ, et al. Enhanced CO_2 photoreduction by a visible-light driven inorganic heterojunction. Energy Environ Sci 2013. in revision.
[5] Hara M, Hasei H, Yashima M, Ikeda S, Takata T, Kondo JN, et al. Mechano-catalytic overall water splitting (II) nafion-deposited Cu_2O. Appl Catal A Gen 2000;190:35–42.
[6] Hara M, Kondo T, Komoda M, Ikeda S, Kondo NJ, Domen K, et al. Cu_2O as a photocatalyst for overall water splitting under visible light irradiation. Chem Commun 1998:357–8.
[7] Kirfel A, Eichhorn K. Accurate structure analysis with synchrotron radiation. The electron density in Al_2O_3 and Cu_2O. Acta Crystallogr Sect A 1990;46:271–84.
[8] Liu Q, Zhou Y, Kou J, Chen X, Tian Z, Gao J, et al. High-yield synthesis of ultralong and ultrathin Zn_2GeO_4 nanoribbons toward improved photocatalytic reduction of CO_2 into renewable hydrocarbon fuel. J Am Chem Soc 2010;132:14385–7.
[9] Narayanan R, El-Sayed MA. Catalysis with transition metal nanoparticles in colloidal solution: nanoparticle shape dependence and stability. J Phys Chem B 2005;109:12663–76.
[10] Pan J, Liu G, Lu GQ, Cheng H-M. On the true photoreactivity order of {001}, {010}, and {101} facets of anatase TiO_2 crystals. Angew Chem Int Ed 2011;50:2133–7.
[11] Paracchino A, Laporte V, Sivula K, Grätzel M, Thimsen E. Highly active oxide photocathode for photoelectrochemical water reduction. Nat Mater 2011;10:456–61.
[12] Raebiger H, Lany S, Zunger A. Origins of the p-type nature and cation deficiency in Cu_2O and related materials. Phys Rev B 2007;76:045209.

[13] Ruiz E, Alvarez S, Alemany P, Evarestov RA. Electronic structure and properties of Cu_2O. Phys Rev B 1997;56:7189–96.
[14] Shiroishi H, Nukaga M, Yamashita S, Kaneko M. Efficient photochemical water oxidation by a molecular catalyst immobilized onto metal oxides. Chem Lett 2002;31:488–9.
[15] Siegfried MJ, Choi K-S. Elucidating the effect of additives on the growth and stability of Cu_2O surfaces via shape transformation of pre-grown crystals. J Am Chem Soc 2006;128:10356–7.
[16] Siriwardane RV, Poston JA. Characterization of copper oxides, iron oxides, and zinc copper ferrite desulfurization sorbents by X-ray photoelectron spectroscopy and scanning electron microscopy. Appl Surf Sci 1993;68:65–80.
[17] Somorjai GA, Blakely DW. Mechanism of catalysis of hydrocarbon reactions by platinum surfaces. Nature 1975;258:580–3.
[18] Tang J, Durrant JR, Klug DR. Mechanism of photocatalytic water splitting in TiO_2. reaction of water with photoholes, importance of charge carrier dynamics, and evidence for four-hole chemistry. J Am Chem Soc 2008;130:13885–91.
[19] Tian N, Zhou Z-Y, Sun S-G, Ding Y, Wang ZL. Synthesis of tetrahexahedral platinum nanocrystals with high-index facets and high electro-oxidation activity. Science 2007;316:732–5.
[20] Wang X, Yin L, Liu G, Wang L, Saito R, Lu GQ, et al. Polar interface-induced improvement in high photocatalytic hydrogen evolution over ZnO-CdS heterostructures. Energy Environ Sci 2011;4:3976–9.
[21] Zeng JH, Jin BB, Wang YF. Facet enhanced photocatalytic effect with uniform single-crystalline zinc oxide nanodisks. Chem Phys Lett 2009;472:90–5.
[22] Zhang Y, Deng B, Zhang T, Gao D, Xu A-W. Shape effects of Cu_2O polyhedral microcrystals on photocatalytic activity. J Phys Chem C 2010;114:5073–9.
[23] Zheng Z, Huang B, Wang Z, Guo M, Qin X, Zhang X, et al. Crystal faces of Cu_2O and their stabilities in photocatalytic reactions. J Phys Chem C 2009;113:14448–53.
[24] Zou Z, Arakawa H. Direct water splitting into H_2 and O_2 under visible light irradiation with a new series of mixed oxide semiconductor photocatalysts. J Photochem Photobiol A 2003;158:145–62.